

PACS numbers: 42.62.Fi; 42.65.Re; 79.60.Fr
DOI: 10.1070/QE2009v039n07ABEH014130

Ultrafast polarisation spectroscopy of photoinduced charges in a conjugated polymer

A.A. Bakulin, D.Yu. Parashchuk, P.H.M. van Loosdrecht, M.S. Pshenichnikov

***Abstract*. Tunable optical parametric generators and amplifiers (OPA), proposed and developed by Akhmanov and his colleagues, have become the working horses in exploration of dynamical processes in physics, chemistry, and biology. In this paper, we demonstrate the possibility of using ultrafast polarisation-sensitive two-colour spectroscopy, performed with a set of two OPAs, to study charge photogeneration and transport in conjugated polymers and their donor-acceptor blends.**

Keywords: *conjugated polymers, ultrafast spectroscopy, charge-transfer complex, exciton.*

'All roads began at our doors . . .'
B. Grebenshchikov. *'The sky is getting closer'*

1. Introduction

Almost 50 years ago, Akhmanov and Khokhlov were amongst the first to propose the concept of the optical parametric generator (OPG) [1 – 3]. Only three years later, in 1965, Akhmanov and his colleagues successfully demonstrated optical parametric amplification (OPA) in the near-IR region [4, 5], and soon after developed a widely-tunable OPG and the first picosecond OPG [6]. Already at that time, they envisioned that 'the main applications of tunable oscillators lies in the chemistry of excited molecules and spectroscopy' [6]. It did not take long for this statement to become reality [7, 8]. Since then, thanks to breathtaking advances in femtosecond technology [9] and nonlinear crystal development [10], OPGs and OPAs have become unique research tools combining incredible (down to 5 fs [11]) time resolution with outstanding spectral tunability (from visible to far-IR spectral ranges [12]). Nowadays, a researcher can either easily build an OPA from the scattered components lying around in the optical lab, or just purchase a commercial one. Both experimental approaches are exploited in the current study where femtosecond OPAs – generating visible and mid-IR light – are used in the spectroscopy of the fundamental chemical processes of charge photogeneration and recombination in organic photovoltaics.

Recent progress in organic photovoltaics has resulted in polymer-fullerene solar cells with energy conversion efficiencies in the range from 4 % to 6 % [13 – 15]. The critical process for solar cell performance is the conversion of light into mobile charges which occurs on a sub-nanosecond timescale. Moreover, geminate recombination of charges after photogeneration can substantially decrease the efficiency of the photon-to-charge conversion. Therefore, charge transport within the first 10 – 100 ps after photogeneration also plays a significant role in the performance of the organic photovoltaic devices. The typical timescales of the above-mentioned processes are inaccessible for the majority of conventional techniques such as, for instance, photocurrent spectroscopy. In contrast, optical probes can access information about the dynamics of photoexcited states at even shorter timescales.

A natural way to study the early charge dynamics in donor-acceptor blends is photoinduced absorption spectroscopy (PIA) [16]. The PIA approach is built upon the fact that the surplus charge on a conjugated molecule induces newly allowed states inside its optical gap thereby forming additional absorption bands in the IR and near-IR spectral ranges. The well-known fingerprints of charged states in the widely-studied conjugated polymer MEH-PPV are the so-called low energy (LE) and high energy (HE) polaron absorption bands at ~ 0.5 eV and 1.3 eV, respectively [17] (following the established terminology, we will call them 'polaron states').

The time-resolved version of PIA has been realised by utilising picosecond [18] and sub-picosecond [19, 20] OPAs to study dynamical photophysical processes in organic light-harvesting systems. In essence, this experimental approach requires two time-synchronised OPGs: one provides photo-excitation pulses in the visible region to mimicl the solar photons, while the other generates a delayed probe pulse to monitor the time-dependent concentration of the photo-generated charges by interrogating the aforementioned charge-induced PIA bands in the IR region. An additional option whose potential is still to be exploited in organic photovoltaics is the polarisation-sensitive version of PIA, where the change of the polarisation state [21] of the IR

A.A. Bakulin, P.H.M. van Loosdrecht, M.S. Pshenichnikov Zernike Institute for Advanced Materials, University of Groningen, Nijenborgh 4, 9747 AG Groningen, the Netherlands; e-mail: A.A.Bakulin@RuG.nl, p.h.m.van.loosdrecht@rug.nl, M.S.Pchenitchnikov@RuG.nl;
D.Yu. Parashchuk Department of Physics, M.V. Lomonosov Moscow State University; International Laser Center, M.V. Lomonosov Moscow State University, Vorob'evy gory, 119991 Moscow, Russia;
e-mail: paraschuk@yandex.ru

Received 27 April 2009
Kvantovaya Elektronika **39** (7) 643 – 648 (2009)
Translated by A.A. Bakulin

probe is observed, thereby providing valuable information on the localisation of the photoexcited states. However, untill now, this technique has not been widely used for studying dynamics of polaron states in conjugated polymers.

In this paper we show how multicolour ultrafast spectroscopy can be used to evaluate the charge-generation efficiency in three different blends of a conjugated polymer with organic acceptors. Moreover, we demonstrate that polarisation-sensitive ultrafast pump-probe experiments can provide additional information about the localisation of photoexcited states in the conjugated polymer.

2. Samples

We studied blends of the conjugated poly[2-methoxy-5-(2'-ethyl-hexyloxy)-1,4-phenylene vinylene] (MEH-PPV) polymer with three organic acceptors: 1,5-dinitroantraquinon (DNAQ), 2,4,7-trinitrofluorenone (TNF), and the soluble derivative of fullerene C_{60} (PCBM). During the preparation, each component was separately dissolved in chlorobenzene at the concentration of 2 g L^{-1}. Then the solutions of the polymer and acceptor were mixed with a weight ratio 1 : 0.3 in the case of DNAQ and TNF, and 1 : 0.2 in the case of fullerene. Films were prepared by drop-casting on CaF_2 substrates which typically resulted in $\sim$ 200-nm-thick films.

Figure 1 compares optical absorption spectra of the donor polymer (MEH-PPV) and donor-acceptor blends (MEH-PPV – fullerene, MEH-PPV – DNAQ, MEH-PPV – TNF). The absorption spectra of the acceptors are not shown because their extinction coefficients are negligibly small in this spectral range. The absorption spectrum of the MEH-PPV – fullerene blend is a superposition of the individual absorption spectra of MEH-PPV and fullerene. On the other hand, MEH-PPV – DNAQ and MEH-PPV – TNF blends display a red shift of the MEH-PPV main absorption band and an additional absorption shoulder extending deeply into the optical gap of MEH-PPV. These changes are associated with the weak donor-acceptor charge-transfer complex (CTC) formation in the blends [22, 23].

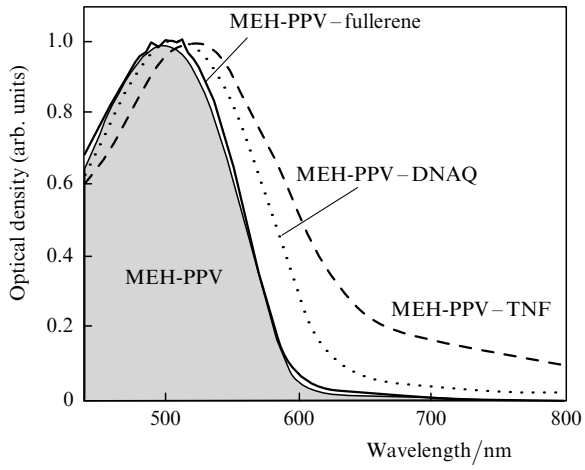

Figure 1. Normalised absorption spectra of the samples under study: MEH-PPV polymer (shaded contour), and donor-acceptor blends: MEH-PPV – fullerene = 1 : 0.2 (solid curve), MEH-PPV – DNAQ = 1 : 0.3 (dotted curve), and MEH-PPV – TNF = 1 : 0.3 (dashed curve).

3. Experimental

Time and spectrally resolved PIA experiments were performed using two setups optimised for wide-range IR tunability, and for high time resolution, respectively. The first system was based on a commercially available Ti : sapphire regenerative amplifier system (Hurricane, Spectra-Physics) and two optical parametric amplifiers (TOPAS, Light Conversion) operating in the visible (500 – 700 nm) and IR (1.3 – 20 μm) regions. The output of the former was used as a pump while the latter provided the tunable IR probe. The polarisations of the pump and probe beams were always parallel. The cross-correlation width for any wavelength combination did not exceed 400 fs.

The second laser system featured a substantially higher time resolution (< 100 fs) and a better signal-to-noise ratio at the expense of IR tunability [24]. A home-built Ti : sapphire multipass amplifier was used to pump a noncollinear optical parametric amplifier providing tunable visible excitation pulses (40 fs, 1 μJ per pulse) and an optical parametric amplifier providing the IR probe [25]. 50-nJ probe pulses, with a duration of $\sim$ 70 fs and a bandwidth of $\sim$ 300 cm^{-1} FWHM, were positioned in the center of the LE polaron peak at 3300 cm^{-1}. The polarisation of the IR probe beam was rotated by 45° with respect to the polarisation of the visible pump beam. After the sample, the probe component parallel or perpendicular to the pump was selected by a wire-grid polariser (extinction 1 : 100) and detected with a liquid-nitrogen-cooled InSb photodiode. All time-resolved PIA data were obtained at temperature 293 K in nitrogen atmosphere.

In the polarisation-sensitive measurements, the isotropic signal ΔT_{iso} and the induced anisotropy $r(t)$ were calculated from the parallel and perpendicular signals using the equations [26]:

$$\Delta T_{iso}(t) = \frac{\Delta T_{||}(t) + 2\Delta T_{\perp}(t)}{3}, \quad (1)$$

$$r(t) = \frac{\Delta T_{||}(t) - \Delta T_{\perp}(t)}{3\Delta T_{iso}(t)}, \quad (2)$$

where $\Delta T_{||}$ and $\Delta T_{\perp}$ stand for the relative transmission changes in the parallel and perpendicular components of the probe, respectively. For non-interacting dipoles in an isotropic medium, the anisotropy decays from its initial value of 0.4 to 0, when the dipoles orientations are completely scrambled by, for instance, motional dynamics. In the isotropic signal, the effect of the dipole reorientation is completely removed thereby showing only population relaxation.

4. Results

Figure 2 presents a typical time and spectrally resolved response of MEH-PPV–DNAQ CTC after excitation into the charge-transfer band at 650 nm. After the excitation, pronounced absorption bands are formed at frequencies 1000 and 3000 cm^{-1}. The low energy band is attributed to the photoinduced changes in the transition dipole moment of the MEH-PPV IR active vibrational modes (also known as IRAVs [19, 27]). The 3000-cm^{-1} band is associated with the formation of polaron states in the polymer leading to low-energy (LE) electronic transitions within the band gap

[17] (see inset in Fig. 2). The third polaron band, the so-called high-energy (HE) band at ~ 1.3 eV, is outside the probe spectral window. After their formation, the amplitudes of both IRAV and LE PIA bands starts decaying with identical time constants. This indicates a similar origin of both spectral features, namely, modification of the polymer band structure by a surplus photoinduced charge.

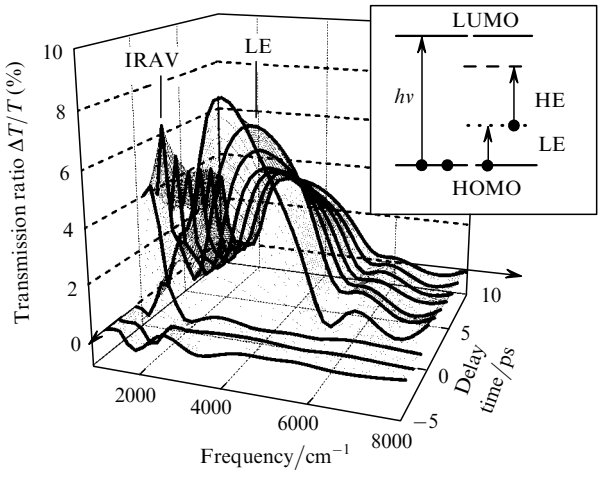

Figure 2. Transient PIA spectra of the MEH-PPV – DNAQ CTC after 650-nm excitation with indicated IR active vibrations (IRAV) of MEH-PPV and low-energy (LE) polaron band. The high-energy (HE) polaron band at ~ 10000 cm^{-1} is outside the probe spectral region. The inset shows the energy diagram of polaron excitations. HOMO (LUMO) is the highest (lowest) occupied (unoccupied) molecular orbital. Black circles represent occupation of molecular orbitals corresponding to the ground and polaron states. Arrows indicate optically allowed transitions.

The transient signals do not exhibit any spectral dynamics, for instance, shifts of the maxima and/or broadening of the spectra. Therefore, we can safely assume that transient changes in the absorption cross-section of the charge-associated bands are small [24]. In this case, intensity variations in the charge-associated bands directly reflect changes in the concentration of charges in the sample due to charge generation and recombination. Since the LE charge-associated absorption band is the strongest, we will further focus on this band to study the early evolution of photoinduced charges in the polymer.

Figure 3 presents the results of transient PIA experiments for all three donor-acceptor blends used in the study. The polymer – fullerene blend was excited in the polymer absorption band (at 540 nm) and the blends of the polymer with DNAQ and TNF were excited in the CTC absorption band (at 650 nm). In the top panels of Fig. 3, one can see both components of the PIA response directly measured in the experiment. These components correspond to different polarisations of the probe pulse: parallel or perpendicular to the pump. The substantial difference in the amplitudes of parallel and perpendicular components indicates a considerable anisotropy of the PIA response. In other words, there is a significant correlation in the orientation of dipole moments between the excitonic (pump) and polaronic (probe) transitions. We will show later on, that the very existence of such a correlation provides incredible opportunities to study localisation and migration of the charged states [24, 28]. On the other hand, the anisotropy of the response should be taken into account when evaluating the concentration of the photoinduced charges from the PIA signals.

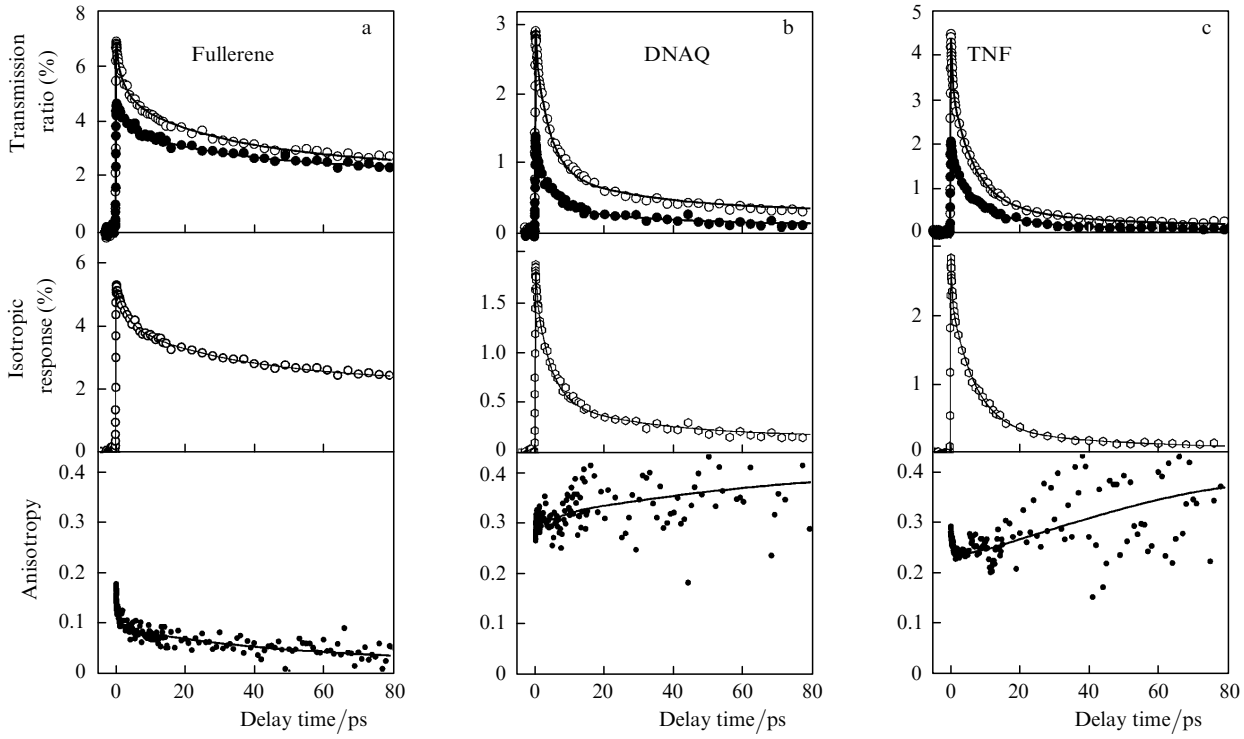

Figure 3. PIA transients for the MEH-PPV – fullerene blend after excitation at 540 nm (a), and for MEH-PPV – DANQ (b), MEH-PPV – TNF (c) blends after excitation at 650 nm. Top panels: experimental PIA transients measured in parallel (open circles) and perpendicular (crossed circles) polarisations between the pump and probe beams. Middle and bottom panels show isotropic responses and transient anisotropies recalculated according to equations (1) and (2), respectively. Symbols and solid curves show experimental data points and the best fits (see the text), respectively.

Table 1. Parameters of the fit to the experimental data with the model presented in Fig. 3.

Acceptor	Isotropic PIA component				Anisotropy			
	$A_1(T_1)$	$A_2(T_2)$	$A_3(T_3)$	A_0''	r_0	$a_1(\tau_1)$	$a_2(\tau_2)$	r_0''
TNF	0.31 (0.3 ps)	0.43 (5.8 ps)	0.26 (22 ps)	0.03	0.29	0.2 (0.7 ps)	0.8 (0.6 ns)	0.4
DNAQ	0.32 (0.3 ps)	0.45 (3.5 ps)	0.23 (35 ps)	0.08	0.29	–	0.95 (> 1 ns)	0.4
Fullerene	0.22 (3.5 ps)	0.31 (30 ps)	0.47 (> 1 ns)	–	0.18	0.53 (0.5 ps)	0.47 (50 ps)	–

Middle panels in Fig. 3 show the evolution of the isotropic response for all samples, calculated with equation (1). In all samples, the PIA response was observed immediately after the photoexcitation which corresponds to instantaneous (within the experimental time resolution) charge photogeneration. After this, the PIA magnitude begins to decay, which is associated with decreasing concentration of charges due to their recombination. The MEH-PPV – fullerene blend demonstrates a rather modest decline of the PIA response during the first 100 ps and, therefore, most of the charges can be considered 'long-lived' (Table 1). In contrast, the PIA kinetics for the blends with TNF and DNAQ show a fast decay which demonstrates the efficient recombination of photogenerated charges. Only a small fraction of the polaron states (10 % and 5 % for DNAQ and TNF, respectively) survives for longer then 100 ps.

The anisotropy transients recalculated from the experimental data according to equation (2) are shown in the bottom panels of Fig. 3. In the MEH-PPV – fullerene blend the anisotropy value right after excitation is relatively low (~ 0.17). Furthermore, the anisotropy substantially decays after the excitation, on the timescales of 0.5 ps and 50 ps. The low anisotropy level indicates that the PIA response corresponds to the polaron transitions with the dipole moments that, on average, substantially deviate from the dipole moment of the excitonic transition. The angle between polaron and exciton dipole moment within a single conjugation segment does not exceed 20° (see below). The rotational and torsion dynamics of polymer chains are strongly inhibited in the film and, therefore, changes in the chromophor conformation can not be responsible for the depolarisation on a picosecond timescale. Therefore, the low anisotropy level indicates that the initially excited and probed transitions correspond to different chromophores (polymer conjugated segments). In other words, the excited state can quickly delocalise from the initially excited molecule. The two different timescales observed in the anisotropy decay imply two different mechanisms of delocalisation. On the basis of previous works [28, 29] we suggest that the fast (< 0.5 ps) depolarisation component corresponds to the exciton transfer between the polymer segments while the slow (50 ps) component originates from the diffusion of the polaron states.

The anisotropy in the blend with a pronounced CTC formation (MEH-PPV – TNF and MEH-PPV – DNAQ) is persistently higher then in the MEH-PPV – fullerene blend (Figs 3b, c). For instance, the initial value of the anisotropy $r_0 \approx 0.3$ is close to the theoretically maximum level of 0.4. The difference between these two values provides the estimate for the maximal angle between dipole moments of excitonic and polaronic transitions. The initial anisotropy value of $r_0 \approx 0.3$ corresponds [26] to an average angle of 20° between exciton and polaron dipoles within a single conjugated segment of a polymer chain. It is important to mention that this value is an upper estimate because the initial depolarisation can also be associated with a delocalisation of the excited state within a few polymer conjugation segments [23]. In general, a relatively high anisotropy indicates that the charge separation occurs within the initially photoexcited polymer chain. This matches well Mulliken's model of the CTC which assumes direct charge separation after the excitation into the CTC absorption band [30]. The slight ($\sim 20\,\%$) drop of the anisotropy at a timescale of ~ 1 ps observed only in the MEH-PPV – TNF blend is difficult to attribute to a particular process. This drop can originate from the deformation of the polymer chain involved in the CTC and/or from a partial delocalisation of the polaron states.

The increase in the anisotropy observed in the CTCs on a timescale of $\sim 10 - 100$ ps could have been explained by a spontaneous ordering of the system. However, this explanation contradicts common sense as well as the second law of thermodynamics. Therefore, the anisotropy recovery can not be explained within the frame of a single homogeneous ensemble of dipoles. On the other hand, the observed effect can originate from the interference of the responses from different subensembles. The seeming contradiction arises from the fact that the anisotropy is not an additive quantity and, thus, should be interpreted together with the isotropic response. Below we present a model for the adequate description of the experimental results.

5. Modelling and discussion of anisotropy transients

During the modelling of PIA transients we assumed that the amplitude of the isotropic response is proportional to the concentration of charges in the sample. The overall multitude of charges was partitioned between two subensembles N' and N'':

$$N(t) = N'(t) + N''(t). \tag{3}$$

According to the previously discussed experimental results, the time evolution of the first sub-ensemble was modelled as a sum of exponential decays to represent the concentration of charge and anisotropy of the response, respectively:

$$N'(t) = A_1 \exp(-t/T_1) + A_2 \exp(-t/T_2) + A_3 \exp(-t/T_3), \tag{4}$$

$$R'(t) = r_0[a_1 \exp(-t/\tau_1) + (1 - a_1) \exp(-t/\tau_2)]. \tag{5}$$

Here A_i ($A_3 = 1 - A_1 - A_2$) are the normalised amplitudes; T_i are the population relaxation times; the variable r_0 stands for the initial anisotropy; and a_i and τ_i are the amplitudes and relaxation times of components of the anisotropy signals.

The second ensemble was considered long-lived (at the time scale of our experiment) and possessing a constant anisotropy:

$$N''(t) = A''_0, \tag{6}$$

$$R''(t) = r''_0. \tag{7}$$

In this case, the amplitudes of the parallel $[\Delta T_{||}(t)]$ and perpendicular $[\Delta T_{\perp}(t)]$ polarisation transients can be expressed as:

$$\Delta T_{||}(t) = A\{N'(t)[1 + 2R'(t)] + N''(t)[1 + 2R''(t)]\}, \tag{8}$$

$$\Delta T_{\perp}(t) = A\{N'(t)[1 - R'(t)] + N''(t)[1 - R''(t)]\}, \tag{9}$$

where A is a normalisation coefficient. Making use of equations (1) and (2), we can derive the expressions for the isotropic signal and transient anisotropy:

$$\Delta T_{\mathrm{iso}}(t) = A[N'(t) + N''(t)], \tag{10}$$

$$r(t) = \frac{N'(t)R'(t) + N''(t)R''(t)}{N'(t) + N''(t)}. \tag{11}$$

One can see from equation (10) that the isotropic transient is free of contamination by reorientational dynamics (for instance, reorientation of the transition dipole). In contrast, the anisotropy calculated according to equation (11) is presented by a mixture of purely reorientational and concentration-related contributions. Therefore, in the case of the response from multiple subensembles with dissimilar dynamics, the anisotropy should be analysed considering also the population kinetics.

Considering the complexity of the model, we utilised a global fit procedure which was simultaneously approximating the parallel, perpendicular, and anisotropic components of the response. The corresponding experimental transients were fitted with theoretical curves recalculated from equations (8), (9) and (11) after convolution with the apparatus response function (a Gaussian with a 100-fs FWHM). Inclusion of the anisotropy transients into the fit procedure substantially stabilised the fitting procedure, especially at long delay times where the absolute values of the PIA response are low. The results of the modelling are presented in Table 1 and shown in Fig. 3 by solid curves.

The model utilised for the fitting of the PIA transients in CTCs assumes existence of two different subensembles of charges. Within the framework of the model, all the photogenerated charges demonstrated a high initial anisotropy. Most of them (90 % – 95 %) have the initial anisotropy $r_0 = 0.3$ (most probably due to initial delocalisation) and almost completely recombine during the first 50 ps after excitation. At the same time, a minor fraction of charges (5 % – 10 %) is strongly localised in the low-energy states (traps) and, because of this, has a constant anisotropy of $r'_0 = 0.4$ and a long lifetime. As the contribution from the former subensemble to the response decreases due to recombination, the input from the latter begins to dominate in the anisotropy dynamics. This explains the experimentally observed growth of average anisotropy at a long timescale (Fig. 3b, c).

6. Conclusions

In this paper we have shown that ultrafast spectroscopy can be used for investigation of charge dynamics in donor-acceptor blends of conjugated polymers. The isotropic component of the PIA response reflects the concentration of charges at the polymer chains. The initial level of transient anisotropy indicates the degree of localisation of the photoexcited states. At the same time, interpretation of anisotropy dynamics at longer (tens of picoseconds) timescales is complicated due to the nonadditive character of the anisotropy. Therefore, in case of a strongly inhomogeneous distribution of polaron states, the isotropic and anisotropic transients should be analysed simultaneously.

Acknowledgements. We thank V.V. Krasnikov for many fruitful discussions. D. Fishman and M. Donker are acknowledged for their assistance in handling the TOPAS OPAs. This study was in part financially supported by the Russian Foundation for Basic Research (Project No. 08-02-12170-ofi).

The authors dedicate this paper to the memory of S.A. Akhmanov; and one of them (M.S.P.) would like to make several personal notes.

I had honour first to graduate and then to work at the Chair of General Physics and Wave Processes headed by S.A. Akhmanov from 1979 to 1991. In fact, I – at that time a 2nd year student of the Department of Physics at the Moscow State University – was taken by S.A. to the Chair, literally by hand after one of his brilliant lectures on physical optics. At that moment, in the lab of late D.P. Krindach I was for the first time acquainted with ultrafast lasers. A few years later, I was tremendously inspired by Akhmanov's public lecture at the 'Scientist's House' which was dedicated to nonlinear optical spectroscopy and the unique information on matter which this spectroscopy can provide. These two words, 'ultrafast' and 'spectroscopy', inspired by S.A., became the keys of my scientific career. Even now, 20 years later, I still frequently visit the Chair in Moscow to feel the unique 'Akhmanov' atmosphere and to touch the doors (see the epigraph) through which my journey into the world of science began.

References

1. Akhmanov S.A., Khokhlov R.V. *Zh. Eksp. Teor. Fiz.*, **43**, 351 (1962).
2. Kingston R.H. *Proc. IRE*, **50**, 472 (1962).
3. Giordmai J.A., Miller R.C. *Phys. Rev. Lett.*, **14**, 973 (1965).
4. Akhmanov S.A., Kovrigin A.I., Piskarkas A.S., Fadeev V.V., Khokhlov R.V. *Pis'ma Zh. Eksp. Teor. Fiz.*, **2**, 300 (1965).
5. Akhmanov S.A., Dmitriev V.G., Kovrigin A.I., Khokhlov R.V. *Phys. of Quantum Electronics Conf. Proc.* (1965).
6. Akhmanov S.A., Kovrigin A.I., Kolosov V.A., Piskarkas A.S., Fadeev V.V., Khokhlov R.V. *Pis'ma Zh. Eksp. Teor. Fiz.*, **3**, 241 (1966).
7. Akmanov A.G., Akhmanov S.A., Khokhlov R.V., Kovrigin A.I., Piskarskas A.S., Sukhorukov A.P. *IEEE J. Quantum Electron.*, **4**, 828 (1968).
8. Akhmanov S.A., Khokhlov R.V. *Usp. Fiz. Nauk*, **88**, 439 (1966).
9. Akhmanov S.A., Vysloukh V.A., Chirkin A.S. *Optics of Femtosecond Laser Pulses* (New York: Amer. Inst. of Physics, 1992).
10. Dmitriev G., Gurzadyan G.G., Nikogosyan D.N. *Handbook of Nonlinear Optical Crystals* (Berlin: Springer, 1991).
11. Baltuska A., Fuji T., Kobayashi T. *Opt. Lett.*, **27**, 306 (2002).
12. Cerullo G., De Silvestri S. *Rev. Sci. Instr.*, **74**, 1 (2003).

13. Peet J., Kim J.Y., Coates N.E., Ma W.L., Moses D., Heeger A.J., Bazan G.C. *Nature Mater.*, **6**, 497 (2007).
14. Kim J.Y., Lee K., Coates N.E., Moses D., Nguyen T.-Q., Dante M., Heeger A.J. *Science*, **317**, 222 (2007).
15. Parashchuk D.Yu., Kokorin A.I. *Ros. Khim. Zh.*, **LII**, 107 (2008).
16. Sariciftci N.S., Smivowits L., Wu R., Gettinger C., Heeger A.J., Wuld F. *Phys. Rev. B*, **47**, 13835 (1992).
17. Wei X., Vardeny Z.V., Sariciftci N.S., Heeger A.J. *Phys. Rev. B*, **53**, 2187 (1996).
18. Akhmanov S.A., Borisov A.V., Danelyus R.V., Piskarskas A.S., Razzhivin A.P., Samuilov V.D. *Pis'ma Zh. Eksp. Teor. Fiz.*, **26**, 655 (1977).
19. Moses D., Dogariu A., Heeger A.J. *Chem. Phys. Lett.,* **316**, 356 (2000).
20. Sheng C.-X., Tong M., Singh S., Vardeny Z.V. *Phys. Rev. B*, **75**, 085206 (2007).
21. Akhmanov S.A., Koroteev N.I. *Metody nelineinoi optiki v spektroskopii rasseyaniya sveta* (Methods of Nonlinear Optics in Light Scattering Spectroscopy) (Moscow: Nauka, 1981).
22. Bakulin A.A., Elizarov S.G., Khodarev A.N., Martyanov D.S., Golovnin I.V., Paraschuk D.Yu., Triebel M.M., Tolstov I.V., Frankevich E.L., Arnautov S.A., Nechvolodova E.M. S*ynthetic Metals*, **147**, 221 (2004).
23. Bruevich V.V., Makhmutov T.S., Elizarov S.G., Nechvolodova E.M., Paraschuk D.Yu. *J. Chem. Phys.*, **127**, 104905 (2007).
24. Bakulin A.A., Martyanov D.S., Paraschuk D.Yu., Pshenichnikov M.S., van Loosdrecht P.H.M. *J. Phys. Chem. B*, **112**, 13730 (2008).
25. Yeremenko S., Baltuska A., de Haan F., Pshenichnikov M.S., Wiersma D.A. *Opt. Lett.*, **27**, 1171 (2002).
26. Gordon R.G. *J. Chem. Phys.*, **45**, 1643 (1966).
27. Mizrahi U., Shtrichmana I., Gershoni D., Ehrenfreund E., Vardeny Z.V. *Synthetic Metals*, **102**, 1182 (1999).
28. Muller J.G., Lupton J.M., Feldmann J., Lemmer U., Scharber M.C., Sariciftci N.S., Brabec C.J., Scherf U. *Phys. Rev. B*, **72**, 195208 (2005).
29. Westenhoff S., Beenken W.J.D., Friend R.H., Greenham N.C., Yartsev A., Sundstrom V. *Phys. Rev. Lett.*, **97**, 166804 (2006).
30. Mulliken R.S. *J. Am. Chem. Soc.*, **72**, 600 (1950).